ACS APPLIED MATERIALS & INTERFACES

Research Article

www.acsami.org

Immobilization of Carboxymethylated Polyethylenimine–Metal-Ion Complexes in Porous Membranes to Selectively Capture His-Tagged Protein

Wenjing Ning, Salinda Wijeratne, Jinlan Dong, and Merlin L. Bruening*

Department of Chemistry, Michigan State University, East Lansing, Michigan 48824, United States

Supporting Information

ABSTRACT: Membrane adsorbers rapidly capture tagged proteins because flow through membrane pores efficiently conveys proteins to binding sites. Effective adsorbers, however, require membrane pores coated with thin films that bind multilayers of proteins. This work employs adsorption of polyelectrolytes that chelate metal ions to create functionalized membranes that selectively capture polyhistidine-tagged (His-tagged) proteins with binding capacities equal to those of high-binding commercial beads. Adsorption of functional polyelectrolytes is simpler than previous membrane-modification strategies such as growth of polymer brushes or derivatization of adsorbed layers with chelating moieties. Sequential adsorption of protonated poly(allylamine) (PAH) and carboxymethylated branched polyethylenimine (CMPEI) leads to membranes that bind Ni^{2+} and capture ~60 mg of His-tagged ubiquitin per mL of membrane. Moreover, these membranes enable isolation of His-tagged protein from cell lysates in <15 min. The backbone amine groups in CMPEI likely increase swelling in water to double protein binding compared to films composed of PAH and the chelating polymer poly[(*N*,*N*-dicarboxymethyl)allylamine] (PDCMAA), which has a hydrocarbon backbone. Metal leaching from PAH/CMPEI- and PAH/PDCMAA-modified membranes is similar to that from GE Hitrap FF columns. Eluates with 0.5 M imidazole contain <10 ppm of Ni^{2+}.

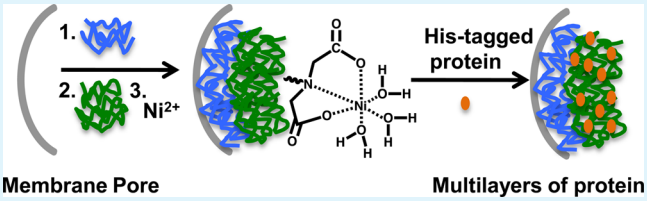

KEYWORDS: *layer-by-layer deposition, His-tagged protein, membrane adsorbers, polyelectrolytes, chelation*

1. INTRODUCTION

In most studies of overexpressed proteins, purification employs engineered affinity tags.[1] Hexahistidine is the most common affinity tag because it is relatively small and enables convenient capture by binding to beads containing Ni^{2+} or Co^{2+} complexes.[2,3] Nevertheless, bead-based separations suffer from slow diffusion of large macromolecules into nanopores,[4−7] which necessitates long separation times that may harm sensitive proteins. Purifications are especially time-consuming when capturing proteins from large volumes of dilute solutions. Porous membranes modified with affinity ligands are an attractive alternative purification platform because convection through the membrane pores and short radial diffusion distances provide rapid protein transport to binding sites.[8,9] Moreover, membrane pressure drops are low because of small thicknesses.[10−14] However, membranes have a lower specific surface area than nanoporous beads, which often leads to a low binding capacity.

To increase protein-binding capacities, several groups modified membrane pores with thin polymer films. Both surface-initiated growth of polymer brushes and layer-by-layer (LbL) polyelectrolyte adsorption can provide highly swollen films that capture multiple layers of proteins.[5,15−21] Compared to the synthesis of polymer brushes, which is a relatively cumbersome process that frequently requires initiator immobilization and subsequent polymerization under anaerobic conditions, LbL deposition is quite simple. Our group employed LbL adsorption of poly(acrylic acid) (PAA)/(polyethylenimine) (PEI) films followed by derivatization with aminobutyl nitrilotriacetate (NTA) and Ni^{2+} to form NTA-Ni^{2+} complexes that capture His-tagged proteins.[22] However, derivatization represents more than 95% of the cost of chemicals and materials for creating protein-binding membranes, and most of the aminobutyl NTA does not couple to the membrane. These expensive reagents may make such membranes impractical. Moreover, in addition to NTA, these membranes contain residual −COOH groups of PAA that bind metal ions only weakly, which leads to metal-ion leaching.

This study examines whether direct adsorption of relatively inexpensive polyelectrolytes containing chelating groups effectively modifies membranes to bind metal ions and capture His-tagged protein (Figure 1). Specifically, we adsorb protonated poly(allylamine) (PAH)/poly[(*N*,*N*-dicarboxymethyl)allylamine] (PDCMAA) or PAH/carboxymethylated branched polyethylenimine (CMPEI) films in membrane pores in ~40 min. Both PDCMAA and CMPEI contain iminodiacetic acid groups that form during reaction of the commercial polymers PAH or branched PEI with sodium

Received: October 31, 2014
Accepted: January 9, 2015
Published: January 9, 2015

DOI: 10.1021/am507607j
ACS Appl. Mater. Interfaces 2015, 7, 2575−2584

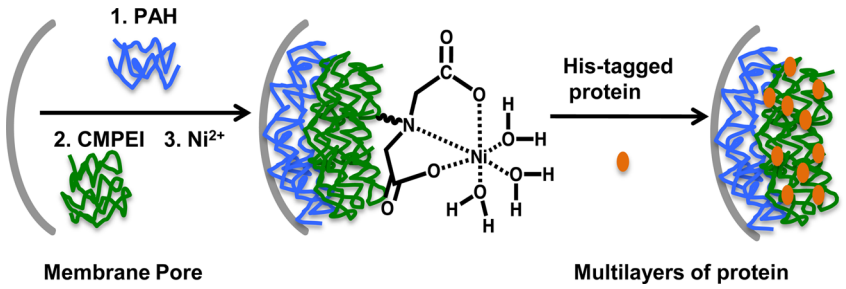

Figure 1. Assembly of a (PAH/CMPEI)-Ni^{2+} film in a nylon membrane pore, and capture of multilayers of His-tagged protein.

Scheme 1. Synthesis of PDCMAA and CMPEI

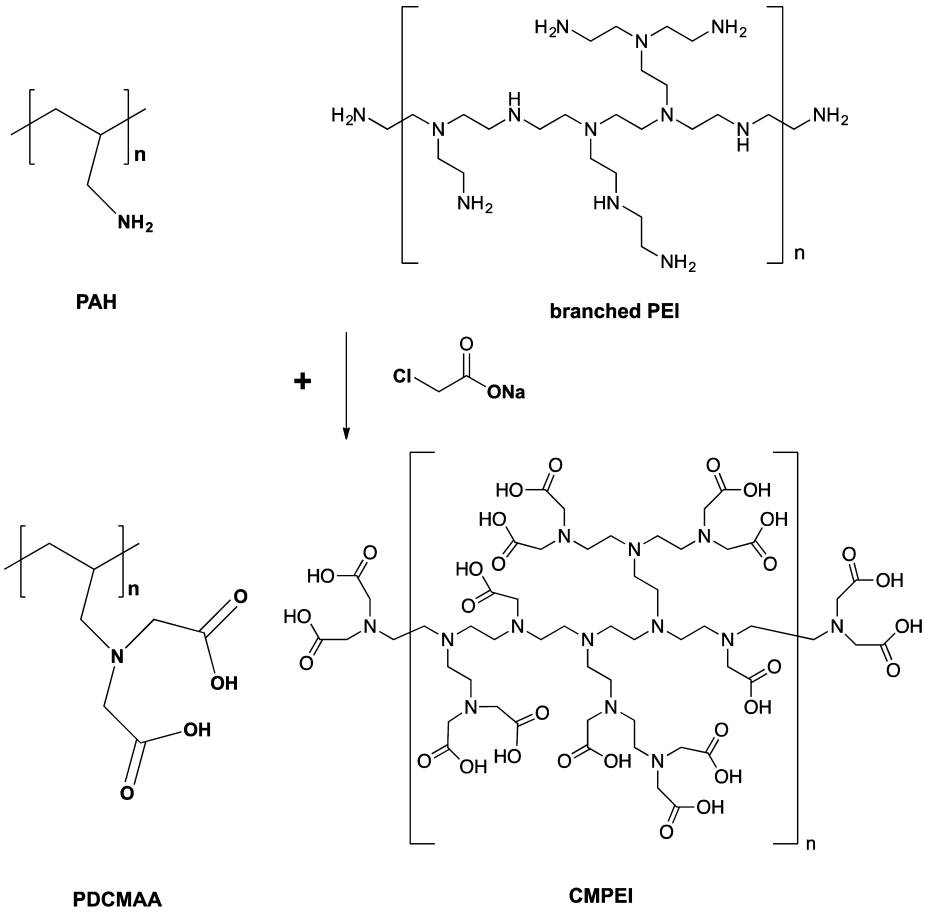

chloroacetate (Scheme 1).[23] Thus, these polymers are readily accessible synthetically and relatively inexpensive. Previous studies examined LbL adsorption of $(PAH/PDCMAA)_n$ films and showed that they can contain up to 2.5 M metal ions and facilitate selective metal-ion transport.[24,25] Carboxymethylated linear PEI is commercially available, but we employ branched PEI because it may provide thicker, highly swollen films for protein capture.[26] Importantly, we compare protein binding to PAH/PDCMAA and PAH/CMPEI films to test our hypothesis that ammonium groups in the PEI backbone will increase swelling and enhance protein capture. Membranes modified with PAH/CMPEI rapidly capture as much as 60 mg of protein per mL of membrane, which is equivalent to the capacities of high-binding commercial beads.[27,28]

2. EXPERIMENTAL SECTION

2.1. Materials. The synthesis of PDCMAA was published previously,[23,25] and the Supporting Information describes the synthesis of CMPEI (Scheme 1) and provides IR spectra (Figure S1, Supporting Information) and elemental analysis. Aqueous solutions containing 0.02 M PAH, 0.01 M CMPEI, or 0.01 M PDCMAA were prepared in deionized water (18.2 MΩ·cm, Milli-Q) or 0.5 M aqueous NaCl, and solution pH values were adjusted by dropwise addition of 0.1 M NaOH or HCl. Polymer concentrations are given with respect to the repeating unit. Au-coated Si wafers (200 nm of sputtered Au on 20 nm of Cr on Si (100) wafers) were cleaned in a UV/O_3 chamber for 15 min prior to use. Other materials include hydroxylated nylon (LoProdyne LP, Pall, 1.2 μm pore size, 110 μm thick), Conconavalin A (Con A from *Canavalia ensiformis* (Jack bean), Sigma-Aldrich), coomassie protein assay reagent (Thermo Scientific), $histidine_6$-tagged ubiquitin (His-U, human recombinant, Boston Biochem), poly(allylamine hydrochloride) (M_w 120 000−200 000 Da, Alfa Aesar), and poly(sodium 4-styrenesufonate) (PSS, M_w ~ 70 000 Da, Sigma-Aldrich). CMPEI synthesis employed a branched poly(ethylenimine)

DOI: 10.1021/am507607j
ACS Appl. Mater. Interfaces 2015, 7, 2575−2584

solution ($M_n \sim 60\,000$ Da by gel-permeation chromatography, average $M_w \sim 750\,000$ Da by light scattering, 50 wt % in H_2O, Sigma-Aldrich). Cupric sulfate, nickel sulfate, sodium phosphate, sodium phosphate dibasic, ethylenediaminetetraacetic acid disodium salt (EDTA), sodium chloroacetate (98%), 3-mercaptopropionic acid (MPA, 99%), and imidazole (>99%) were received from Aldrich and used without further purification. Buffers include binding buffer 1: 20 mM phosphate, pH 6; binding buffer 2: 20 mM phosphate, pH 7.4; washing buffer 1: 20 mM phosphate, 150 mM NaCl, 0.1% Tween 20, pH 7.4; washing buffer 2: 20 mM phosphate, 45 mM imidazole, 150 mM NaCl, pH 7.4; elution buffer: 20 mM phosphate, 500 mM NaCl, 500 mM imidazole, pH 7.4; stripping buffer: 20 mM phosphate, 500 mM NaCl, 50 mM EDTA, pH 7.4. Unless noted otherwise, uncertainties are standard deviations of values derived from three experiments with independent membranes or wafers.

2.2. Adsorption of Polyelectrolyte Multilayers (PEMs). Au-coated Si substrates (24 × 11 mm) were immersed in 5 mM MPA in ethanol for 16 h, rinsed with ethanol, and dried with N_2 to form a monolayer of MPA for adsorption of PAH. These substrates were immersed in 0.02 M PAH (adjusted to the desired pH) for 15 min and subsequently rinsed with 10 mL of deionized water and blown dry with N_2. Substrates were then immersed in a 0.01 M CMPEI or PDCMAA solution (adjusted to the desired pH value) for 15 min followed by the same rinsing and drying procedures. Adsorption presumably displaces counterions from the polyelectrolytes and creates electrostatic cross-links between PAH and CMPEI or PDCMAA to stabilize the films, despite the high water-solubility of these polymers.[29] In some cases, the polyelectrolyte solutions also contained 0.5 M NaCl. The process was repeated to form multilayer films.

For some experiments, nylon membranes were first immersed in 0.1 M sodium chloroacetate in 3 M NaOH for 16 h and subsequently washed with deionized water and dried with N_2. The resulting carboxymethylated membrane disks were cleaned for 10 min with UV/O_3 and placed in a homemade Teflon holder (similar to an Amicon cell) that exposed 3.1 cm^2 of external membrane surface area. (The UV/O_3 exposure should oxidize contaminants or the surface of the membrane but have minimal effect on the membrane structure.[30] Attenuated total reflection-FTIR spectra show no detectable change in the membrane after UV/O_3 treatment, Supporting Information, Figure S2.) Subsequently, a 5 mL solution containing 0.02 M PAH and 0.5 M NaCl was circulated through the membrane for 15 min at a flow rate of 1 mL/min using a peristaltic pump. A CMPEI or PDCMAA layer was deposited similarly using 0.01 M CMPEI or 0.01 M PDCMAA solutions containing 0.5 M NaCl. After deposition of each polyelectrolyte layer, 20 mL of deionized water was passed through the membrane at the same flow rate. Nylon membranes without carboxymethylation were modified with PEMs similarly, starting with the UV/O_3 cleaning.

2.3. Characterization of Polyelectrolyte Films on Gold-Coated Wafers. Spectroscopic ellipsometry (model M-44; J.A. Woollam) was used to determine the thicknesses of PEMs on gold-coated Si wafers, assuming a film refractive index of 1.5. Film thicknesses in aqueous solutions were measured in a home-built cell described previously.[31] In that case, the software determines the refractive index of swollen films. Reflectance FTIR spectra were obtained with a Thermo Nicolet 6700 FTIR spectrometer using a Pike grazing angle (80°) apparatus. A UV/O_3-cleaned Au-coated Si wafer served as a background.

2.4. Metal-Ion and Protein Binding in $(PAH/CMPEI)_n$- and $(PAH/PDCMAA)_n$-Modified Wafers and Membranes. Bare carboxymethylated membranes and membranes modified with $(PAH/CMPEI)_n$ and $(PAH/PDCMAA)_n$ films were loaded with Cu^{2+} or Ni^{2+} by circulating 5 mL of 0.1 M $CuSO_4$ or $NiSO_4$ (pH ≈ 4 for both) through the membrane for 30 min, followed by passage of 20 mL of water through the membrane. Metal ions were eluted from the membranes with 5 mL of stripping buffer or 2% HNO_3 and subsequently analyzed by atomic absorption spectroscopy (see the Supporting Information for analysis details).

For protein capture on wafers coated with PEMs, the modified substrates were immersed for 1 h in solutions containing 0.3 mg/mL of Con A in binding buffer 1 or 0.3 mg/mL of His-U in binding buffer 2. Subsequently, using a Pasteur pipette, these substrates were rinsed with 10 mL of washing buffer 1 and 10 mL of water for 1 min each and dried with N_2. The amount of protein binding was determined by reflectance Fourier transform infrared (FTIR) spectroscopy and expressed as the equivalent thickness of spin-coated protein that would give the same absorbance. The equivalent thickness, d, is calculated from the difference in absorbance (ΔA) at 1680 cm^{-1} (amide band I of protein) before and after binding, using the equation d (nm) = $\Delta A/0.0017$.[32] Some of these thicknesses were confirmed using ellipsometry. If the protein density is 1 g/cm^3, each nm of equivalent thickness is equal to 1 mg/m^2 of surface coverage.

Protein breakthrough curves were obtained by passing protein solutions (0.3 mg/mL in binding buffer 1 or binding buffer 2) through the membranes. For Con A binding, these studies employed 3.1 cm^2 of external membrane surface area. His-U binding experiments used a Teflon holder that exposed a membrane area of 0.78 cm^2 (1.0 cm exposed diameter) because of the high cost of this protein. Bradford assays (using calibration with the protein of interest) were employed to quantify the concentrations of proteins in the membrane effluent or eluate. Prior to protein elution with 6 mL of stripping buffer or elution buffer, membranes were rinsed with 10 mL of either binding buffer 1 for Con A or binding buffer 2 for His-U.

2.5. Protein Separation from a Cell Extract. His-tagged small ubiquitin modifier (His-SUMO) was overexpressed in *Escherichia coli* (*E. coli*) cells. The cells were lysed with sonication in binding buffer 2 and centrifuged. Supernatant was pumped thorough the (PAH/CMPEI)-modified membrane (diameter 2.0 cm) at room temperature at a flow rate of 1 mL/min. Subsequently, the membrane was rinsed with 5 mL of binding buffer 2 and 5 mL of washing buffer 1, and the bound protein was eluted with 2 mL of elution buffer. The purity of the eluted protein was determined by sodium dodecyl sulfate-polyacrylamide gel electrophoresis (SDS-PAGE).

2.6. Metal Leaching, Film Stability and Film Reusability. To test metal-ion leaching in different buffers, (PAH/PDCMAA)-, $(PAH/PDCMAA)_2$-, (PAH/CMPEI)-, and $(PAH/CMPEI)_2$-modified carboxymethylated nylon membranes were loaded with Ni^{2+} using the above procedure (including rinsing with 20 mL of water) and washed consecutively with 160 bed volumes (5 mL) of binding buffer 2, washing buffer 1, washing buffer 2, elution buffer, stripping buffer, and 2% HNO_3. As a comparison, a GE Healthcare HiTrap IMAC FF column (1 mL) was washed with 160 bed volumes (160 mL) of the same buffers. All the samples were diluted 1:5 with deionized water and analyzed by atomic absorption spectrometry. The GE Healthcare HiTrap IMAC FF column was loaded with Ni^{2+} by passing 2 mL of 0.1 M $NiSO_4$ through the syringe column (flow rate of 1 mL/min) followed by 160 mL of deionized water.

To examine film stability under purification conditions, we soaked $(PAH/CMPEI)_2$-modified gold wafers in 5 mL of binding buffer 2 for 20 h. Film thickness values and reflectance FTIR spectra were obtained before and after immersion in the buffer for different times. Total organic carbon (TOC, O.I. Analytical, Model 1010) analysis was used to quantify polyelectrolyte leaching from modified membranes during passage of binding buffer 2 through the membrane. CMPEI solutions with concentrations from 0 to 10 ppm were used for calibration, and the effluent was diluted 1:39 with deionized water before analysis. To study reusability, multiple cycles of charging with Cu^{2+}, binding of Con A, rinsing, elution, and rinsing with water were performed with (PAH/CMPEI)-modified membranes (deposited at pH 2 with 0.5 M NaCl). Protein binding was calculated from the average of capacities determined from the breakthrough curve and the eluate analysis.

3. RESULTS AND DISCUSSION

3.1. LbL Adsorption of Films Containing CMPEI. CMPEI contains both weakly basic (amine) and weakly acidic (carboxylic acid) groups and thus can potentially form salt bridges with both cations and anions on a surface. An acid titration of CMPEI (Figure S3, Supporting Information)

DOI: 10.1021/am507607j
ACS Appl. Mater. Interfaces 2015, 7, 2575−2584

suggests nearly complete protonation of amine groups at pH values below 7, whereas protonation of the carboxylate groups begins below pH 4, which is similar to the titration of PDCMAA.[25] This is reasonably consistent with the pK_a values for iminodiacetic acid, which are 9.4, 2.6, and 1.8.[33,34] The ratio of carboxylic acid groups to amines is around 1:1 in CMPEI but 2:1 in iminodiacetic acid and PDCMAA (see Scheme 1).

On the basis of the polymer titration and a 1:1 ratio of amine to carboxylic acid groups, one might suppose that CMPEI would serve as a polyanion in films formed at basic pH and as a polycation in films formed at acidic pH. However, Hoffman and Tieke reported that linear CMPEI, which also has a 1:1 ratio of amine to carboxylic acid groups, forms multilayer films with protonated poly(vinyl amine) at adsorption pH values ranging from 2 to 8.[35] Thus, even at pH 2, linear CMPEI likely serves as a polyanion in LbL deposition. With branched CMPEI, adsorption of (polycation/CMPEI)$_n$ coatings also occurs at low pH. Figure 2 shows the ellipsometric thicknesses of (PAH/CMPEI)$_n$ films deposited at pH 3. In the absence of salt in adsorption solutions (red circles), after deposition of the initial bilayer, which is ~1 nm thick, adsorption of each subsequent bilayer adds ~5 nm of thickness. Addition of 0.5 M NaCl to adsorption solutions increases the thicknesses of most layers 2- to 4-fold. At low pH, CMPEI has a net positive charge, so electrostatic repulsion between its positive ammonium groups should make the polymer chains partially extend. Addition of salt increases thickness by screening charges in the polymer to create loops and tails and by increasing surface roughness.[36,37]

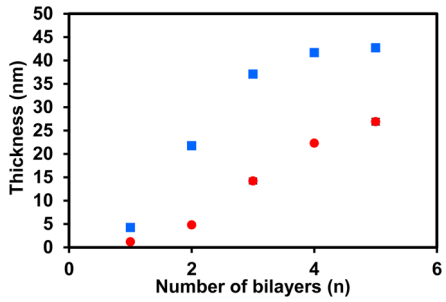

Figure 2. Ellipsometric thicknesses of (PAH/CMPEI)$_n$ films as a function of the number of adsorbed bilayers, n. Films were deposited from pH 3 solutions containing 0.5 M NaCl (blue squares) or no added salt (red circles). The substrates were Au-coated Si wafers modified with a monolayer of MPA, and error bars are typically smaller than the symbols.

During adsorption, carboxylate groups on CMPEI most likely bind to ammonium groups of PAH. Reflectance FTIR spectroscopy confirms that most of the carboxylate groups in these films are deprotonated (Figure 3). Formation of PAH/CMPEI complexes leads to less protonation of the −COOH groups of CMPEI than in solution and perhaps less protonation of ammonium groups. XPS data (Figure S4, Supporting Information) show no chloride within CMPEI-capped films, which suggests that few of the amine groups in CMPEI are protonated and compensated by Cl^- ions. The formation of films by adsorption of CMPEI and PAH, which both possess a net positive charge in neutral and acidic solutions, likely occurs due to polarization-induced attraction.[38−40] Electric fields created by positively charged PAH may induce rearrangement of the CMPEI chains to enhance electrostatic interactions between the carboxylates of CMPEI and ammonium groups of

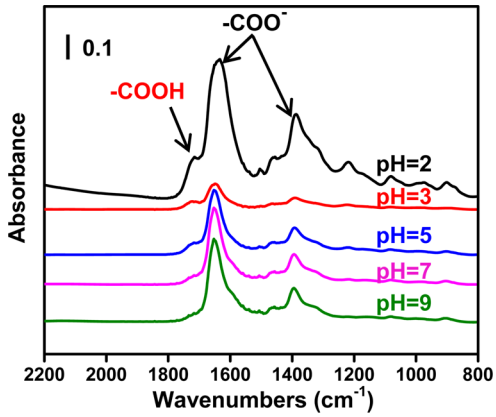

Figure 3. Reflectance FTIR spectra (2200−800 cm^{-1}) of (PAH/CMPEI)$_5$ films deposited at pH 2, 3, 5, 7, or 9 on MPA-modified, Au-coated Si wafers.

PAH. At pH 3 with 0.5 M NaCl, (PAH/CMPEI) growth reaches a plateau at 4−5 bilayers, perhaps because the net positive charge on both polymers leads to repulsions that overcome polarization-induced attraction in thicker films.

Figure 4 shows the thicknesses of (PAH/CMPEI)$_n$ films as a function of the deposition pH. Similar to other films with weak-acid polyelectrolytes,[25,41,42] the highest thicknesses occur with films deposited at the lowest pH. Films formed at pH 2 are typically about 2 times as thick as films adsorbed at pH 3−9. Due to the relatively low pK_a values of the −COOH groups in CMPEI, thickness only increases at the lowest pH value. Notably, 4- and 5-bilayer films deposited at pH 3 are thinner than corresponding films deposited at all other pH values (compare Figures 2 and 4). This may reflect repulsion between CMPEI and PAH at this pH. At pH 2, an increased number of protonated −COOH groups may require more CMPEI to form ion pairs with PAH and overcome decreases in thickness due to repulsion between the two polymers.

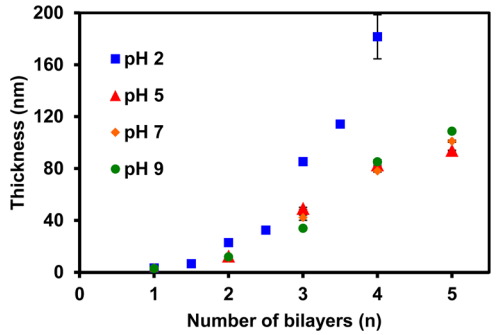

Figure 4. Ellipsometric thicknesses of (PAH/CMPEI)$_n$ films as a function of deposition pH. Films were adsorbed from 0.5 M NaCl solutions onto Au-coated Si wafers modified with a monolayer of MPA, and error bars are often smaller than the symbols. (For coatings adsorbed at pH 2, noninteger bilayer numbers indicate films terminated by PAH adsorption.)

For the pH 2 deposition, we also determined the thickness increases due to adsorption of both PAH and CMPEI. As Figure 4 shows (blue squares), the thickness increase upon adsorption of CMPEI is more than double that for adsorption of PAH, suggesting that the films contain more CMPEI than PAH, probably because the density of $-COO^-$ groups on CMPEI is lower than the density of protonated amine groups

DOI: 10.1021/am507607j
ACS Appl. Mater. Interfaces 2015, 7, 2575−2584

on PAH. After deposition of the fifth (PAH/CMPEI) bilayer at pH 2, the surface is too rough for an accurate thickness determination by ellipsometry.

The reflectance IR spectra of $(PAH/CMPEI)_5$ films deposited at different pH values show that most of the carboxylic groups are deprotonated (Figure 3). However, the ratio of the absorbance of the $-COO^-$ stretch (~1650 cm^{-1}) to the absorbance of the acid carbonyl stretch (1720 cm^{-1}) decreases as the deposition pH decreases, suggesting the films deposited at the lowest pH values contain free −COOH groups. The Supporting Information presents the reflectance FTIR spectra of films with 1 to 5 (PAH/CMPEI) bilayers for different deposition pH values (Figure S5, Supporting Information).

CMPEI gives very thin films when serving as a polycation in LbL adsorption. $(CMPEI/PSS)_5$ films deposited at pH 3 in 0.5 M salt are only 10 ± 2 nm thick. The positive charges of CMPEI reside mostly in or near the backbone and may be less available for adsorption than $-COO^-$ groups on the side chains. Using a cyclic analogue of linear CMPEI, Hoffman and Tieke also found minimal growth during LbL deposition with PSS over a pH range from 2 to 8.[35]

3.2. Film Swelling. This work aims to create thin films that selectively bind proteins in platforms such as porous membranes, and film swelling in aqueous solution is vital to enable extensive protein capture. To examine swelling, we initially performed in situ ellipsometry with $(PAH/CMPEI)_5$ films (deposited at pH 3 with 0.5 M NaCl) immersed in deionized water or binding buffer 2 (pH 7.4). After a 20 min immersion, film thickness increased 160 ± 30% in deionized water and 680 ± 260% in buffer. Consistent with the approximately 62% and 88% water in the immersed coatings, the film refractive indices decrease from 1.50 to 1.39 and from 1.50 to 1.35 after swelling in water and buffer, respectively. (The refractive index of water at the wavelengths of the spectroscopic ellipsometer is about 1.333.) Deprotonation of −COOH groups in pH 7.4 buffer likely enhances swelling, which should provide space for binding multilayers of protein in the film. IR spectra confirm the deprotonation after immersing the film in buffer (see Figure S6, Supporting Information). As a comparison, the swelling of $(PAH/PDCMAA)_5$ films (deposited at pH 3 with 0.5 M NaCl) was 52 ± 16% in deionized water and 220 ± 20% in binding buffer 2. The high swelling of $(PAH/CMPEI)_5$ relative to $(PAH/PDCMAA)_5$ suggests that the ammonium-containing backbone and branched structure of CMPEI facilitate swelling. ($(PAH/CMPEI)_5$ and $(PAH/PDCMAA)_5$ films have similar dry thicknesses of 40 and 60 nm, respectively.) Note that high swelling may lead to partial polyelectrolyte desorption, which we discuss in section 3.8.

Modification of porous membranes to bind proteins will most likely involve adsorption of only a few polyelectrolyte bilayers to simplify the process and avoid plugging of pores. Moreover, the films should contain metal-ion complexes for capture of proteins through metal-ion affinity interactions (Figure 1). Thus, we also examined swelling of $(PAH/CMPEI)_2$ and $(PAH/PDCMAA)_2$ films containing Cu^{2+} complexes. These studies employed binding buffer 1 (pH 6.0) to match subsequent Con A-binding studies, as Con A solutions are not stable at pH 7.4. Figure S7 (Supporting Information) shows that for all film-adsorption pH values (pH 2 to 9), the $(PAH/CMPEI)_2$-Cu^{2+} swelling in pH 6.0 buffer is around 200%. In pH 7.4 buffer, the swelling of a $(PAH/CMPEI)_2$-Cu^{2+} film (deposited at pH 3 with 0.5 M NaCl) is still only 220%. Thus, formation of the metal-ion complexes decreases film swelling, probably because Cu^{2+}-iminodiacetate complexes have no net charge. When immersed in pH 6.0 buffer, the $(PAH/PDCMAA)_2$-Cu^{2+} films show average swellings of only 100% for deposition pH vales of 3, 5, or 7. Although both CMPEI and PDCMAA contain iminodiacetate moieties, the amine or ammonium groups in the backbone of CMPEI films likely increase swelling compared to films with PDCMAA, which contains a hydrocarbon backbone.

3.3. Protein Binding to $(PAH/CMPEI)_2$-Cu^{2+} and $(PAH/PDCMAA)_2$-Cu^{2+} Films. Initial studies of protein binding examined capture of Con A in $(PAH/CMPEI)_2$-Cu^{2+} and $(PAH/PDCMAA)_2$-Cu^{2+} films adsorbed on Au-coated Si wafers modified with MPA. Binding presumably occurs when histidine groups on the protein coordinate with immobilized Cu^{2+}. Using reflectance FTIR spectroscopy, we determine the amount of protein binding based on the amide absorbance, which we compare to the absorbance in spin-coated films with different thicknesses.[32] $(PAH/PDCMAA)_2$-Cu^{2+} films have average thicknesses ranging from 7 to 25 nm, depending on the deposition pH (see Figure 5), but these coatings bind the equivalent of <3 nm of protein, or less than a monolayer. (The dimensions of a Con A protomer, M_w = 25 500 Da, are 4.2 × 4.0 × 3.9 nm.[43]) Even with an extra bilayer, $(PAH/PDCMAA)_3$-Cu^{2+} films with a thickness of ~60 nm (deposited at pH 2) bind only 8 nm of Con A. Such limited binding will lead to low capacities in membranes modified with these films. In contrast, $(PAH/CMPEI)_2$-Cu^{2+} films adsorbed at pH 2 have an average thickness of 48 nm and capture 18 nm of protein (Figure 5). Adsorption of $(PAH/CMPEI)_2$ at deposition pH values from 3 to 7 leads to thinner films than adsorption at pH 2 and binding of ≤5 nm of protein (Figure 5). Thus, polyelectrolyte adsorption at low pH to obtain relatively thick CMPEI films and high swelling is likely vital to achieving high binding capacities.

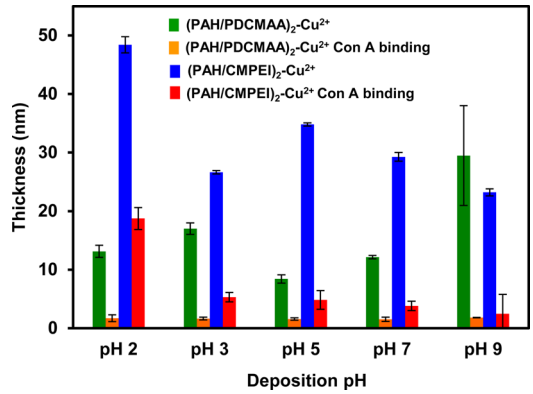

Figure 5. Thicknesses of $(PAH/PDCMAA)_2$ and $(PAH/CMPEI)_2$ multilayers after complexation of Cu^{2+}, and the equivalent thicknesses of Con A subsequently adsorbed in these films. PEMs were deposited from polyelectrolyte solutions containing 0.5 M NaCl at various pH values.

3.4. Membrane Modification with $(PAH/CMPEI)_n$ and $(PAH/PDCMAA)_n$ Films and Binding of Metal Ions. Adsorption of $(PAH/CMPEI)_n$ and $(PAH/PDCMAA)_n$ films within membrane pores is difficult to quantify. To qualitatively assess the amount of adsorbed polymer, we examined Cu^{2+} and Ni^{2+} binding in membranes modified with polyelectrolyte films.

DOI: 10.1021/am507607j
ACS Appl. Mater. Interfaces 2015, 7, 2575−2584

As Figure 6 shows, an untreated nylon membrane modified with PAH/CMPEI (far left data bars) binds <1 mg of Cu^{2+} per

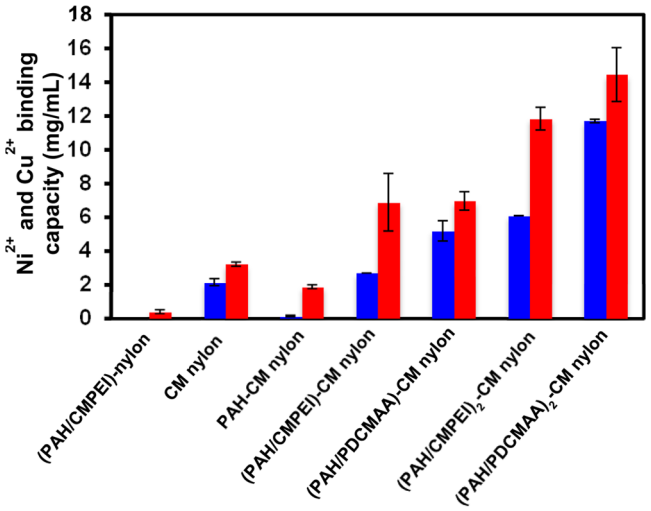

Figure 6. Cu^{2+} (red bars) and Ni^{2+} (blue bars) binding capacities in PAH/CMPEI-modified nylon, carboxymethylated (CM) nylon, PAH-modified CM nylon, PAH/CMPEI-modified CM nylon, PAH/PDCMAA-modified CM nylon, $(PAH/CMPEI)_2$-modified CM nylon, and $(PAH/PDCMAA)_2$-modified CM nylon membranes. All polyelectrolytes were adsorbed at pH 2 from solutions containing 0.5 M NaCl. Error bars are the differences between experiments with two different membranes.

mL of membrane. This implies minimal adsorption of PAH/CMPEI, so we treated the nylon substrates with 0.1 M sodium chloroacetate in 3 M NaOH to increase the number of −COOH groups on pore surfaces and enhance polyelectrolyte adsorption. Unfortunately, in control experiments carboxymethylated (CM) nylon captures 3 mg of Cu^{2+} per mL of membrane. However, adsorption of PAH in the membrane decreases the Cu^{2+} capture to about 2 mg/mL, presumably because PAH forms salt bridges with some COO^- groups to prevent binding. Protonation of the amine groups should prevent them from binding Cu^{2+}. (The pH of the Cu^{2+} loading solution is ~4). Subsequent adsorption of a CMPEI layer leads to capture of 7 mg of Cu^{2+} per mL of membrane, and CM nylon membranes modified with single PAH/CMPEI and PAH/PDCMAA bilayers show similar Cu^{2+} binding. Moreover, $(PAH/CMPEI)_2$- and $(PAH/PDCMAA)_2$-modified CM membranes capture around 12 and 14 mg of Cu^{2+} per mL of membrane, respectively.

Importantly, the PAH/CMPEI-CM nylon membrane binds 16 times the amount of Cu^{2+} captured in an untreated nylon membrane modified with PAH/CMPEI. Figure 7 shows scanning electron microscopy (SEM) images of bare nylon, CM nylon, (PAH/CMPEI)-Cu^{2+} CM nylon, and $(PAH/CMPEI)_2$-Cu^{2+} CM nylon. The structures of the nylon membranes show no obvious change after carboxymethylation, so the primary effect of this treatment is the formation of −COOH groups that facilitate adsorption of the initial PAH layer.

Selective capture of His-tagged proteins typically employs immobilized Ni^{2+} or Co^{2+} complexes, not Cu^{2+}. Histidine binding to Ni^{2+} and Co^{2+} is weaker than to Cu^{2+} and thus requires multiple histidine residues for protein capture, which affords selective sorption of His-tagged species. As Figure 6

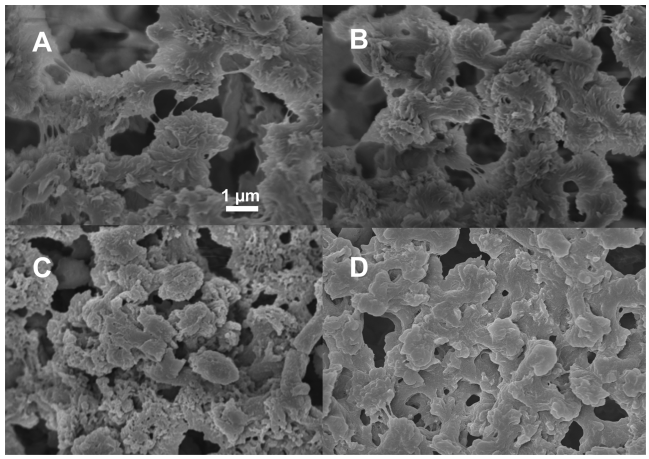

Figure 7. SEM images of (A) nylon, (B) carboxymethylated nylon, (C) PAH/CMPEI-Cu^{2+}-modified carboxymethylated nylon, and (D) $(PAH/CMPEI)_2$-Cu^{2+}-modified carboxymethylated nylon membranes. The scale bar is common to all images.

shows, CM nylon membranes modified with PAH/CMPEI and $(PAH/CMPEI)_2$ films bind 2 and 5 mg/mL of Ni^{2+}, respectively. This is considerably less than the Cu^{2+} binding capacity, perhaps because Ni^{2+} only binds strongly to sites with the full iminodiacetic acid functionality. Amines modified with a single carboxylic acid group (see Scheme 1) may not give stable Ni^{2+} complexes. The unmodified CM nylon also shows less Ni^{2+} binding than Cu^{2+} binding, and CM membranes modified with only PAH show minimal Ni^{2+} capture. PDCMAA contains only IDA binding groups, so there is not a large difference between Ni^{2+} and Cu^{2+} binding to membranes with PAH/PDCMAA films. Hence the membranes modified with PAH/PDCMAA and $(PAH/PDCMAA)_2$ capture more Ni^{2+} than corresponding membranes modified with PAH/CMPEI and $(PAH/CMPEI)_2$. From metal-ion binding, we can estimate the polymer adsorption in a membrane. For (PAH/CMPEI)-modified membranes, the Ni^{2+} (M_w = 58.7 g/mol) binding is around 3 mg/mL. Assuming that only complete IDA groups bind Ni^{2+}, 4 metal ions should bind to the CMPEI repeat unit in Scheme 1. Thus, a (PAH/CMPEI)-modified CM membrane will contain 14 mg/mL of CMPEI (repeat unit M_w = 1112 g/mol).

3.5. Con A Binding to Membranes Modified with PAH/PDCMAA-Cu^{2+} and PAH/CMPEI-Cu^{2+} Films. Due to the high cost of His-tagged proteins, we first employed Con A binding to Cu^{2+} complexes to evaluate the protein-binding capacities of membranes. Figure 8 shows the breakthrough curves for Con A capture in CM nylon membranes modified with PAH/CMPEI-Cu^{2+}(purple circles) and PAH/PDCMAA-Cu^{2+} (green squares) films. Even though both films show similar Cu^{2+} binding (Figure 6), the total Con A bound to the membrane with PAH/CMPEI-Cu^{2+} is 59 ± 5 mg/mL, whereas the membrane with PAH/PDCMAA-Cu^{2+} captures just 30 ± 5 mg/mL. Binding capacities determined from Con A elution with 50 mM EDTA (stripping buffer) are similar to those from the breakthrough curves (55 ± 10 and 35 ± 8 mg/mL for PAH/CMPEI-Cu^{2+} and PAH/PDCMAA-Cu^{2+}, respectively). The higher binding capacity with PAH/CMPEI-Cu^{2+} than PAH/PDCMAA-Cu^{2+} is consistent with the trends in Con A binding capacities of PEM films on Au-coated Si wafers (Figure 5).

DOI: 10.1021/am507607j
ACS Appl. Mater. Interfaces 2015, 7, 2575−2584

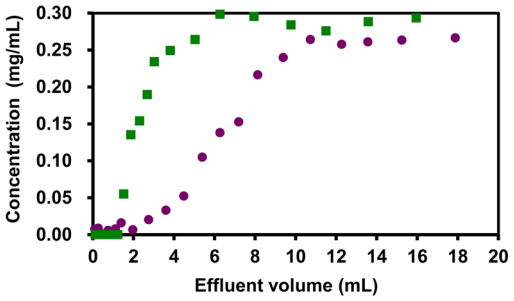

Figure 8. Breakthrough curves of Con A capture in CM nylon membranes (2.0 cm diameter) modified with PAH/CMPEI-Cu^{2+} (purple circles) and PAH/PDCMAA-Cu^{2+} (green squares). Both films were deposited at pH 2 with 0.5 M NaCl. The feed Con A concentration was 0.3 mg/mL and the flow rate was 10 cm/h.

We also tested Con A binding in $(PAH/CMPEI)_2$-Cu^{2+}-modified CM nylon. Based on breakthrough curves (e.g., Figure S8, Supporting Information), the Con A binding capacity in these membranes is 39 ± 5 mg/mL, or less than in membranes with PAH/CMPEI-Cu^{2+} films. The unexpected decrease in binding compared to a film with a single bilayer may reflect decreased swelling with more bilayers or limited access to some small pores after coating the spongy membrane structure (see Figure 7) with two bilayers. Con A capture in membranes modified with $(PAH/PDCMAA)_2$-Cu^{2+} is also less than in membranes with (PAH/PDCMAA)-Cu^{2+} (see Figure S8, Supporting Information).

3.6. Capture of His-Tagged Protein Using Membranes Containing PAH/CMPEI-Ni^{2+} Films. Because they showed the highest Con A capture, we determined the binding capacity for His-tagged ubiquitin using CM nylon membranes modified with PAH/CMPEI films. However, in this case, we employed the Ni^{2+} complex, which is necessary for selective capture of His-tagged protein. Based on breakthrough curves (Figure 9),

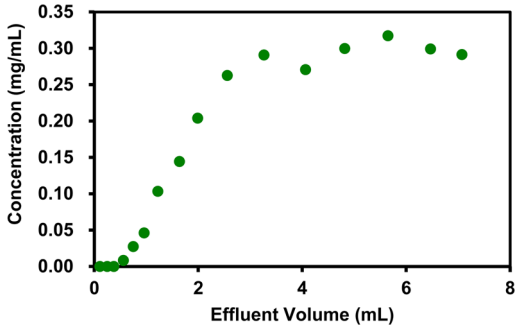

Figure 9. Breakthrough curve for His-tagged ubiquitin capture in a (PAH/CMPEI)-modified CM membrane. The flow rate was 10 cm/h, the membrane had a diameter of 1.0 cm, and the feed His-tagged ubiquitin concentration was 0.3 mg/mL. The His-tagged ubiquitin binding capacity was 55 mg/mL for this membrane and 64 mg/mL for a second replicate membrane.

the binding capacity is ~60 mg/mL, and protein elution in 0.5 M imidazole (elution buffer) gave a capacity of ~70 mg/mL. This His-U binding is about 2/3 of what we previously obtained using polymer brush- or (PAA/PEI/PAA)-NTA-Ni^{2+}-modified membranes (~90 mg/mL membrane).[22,44] However, this new strategy avoids the challenges of growing polymer brushes or the expensive reaction of PAA/PEI/PAA with aminobutyl NTA. The dynamic binding capacity, i.e., the amount of protein bound when the effluent concentration is 10% of the loading concentration, is around 30 mg/mL.

To demonstrate that membranes can isolate His-tagged protein directly from cell extracts, we purified His-tagged SUMO protein that was overexpressed in *E. coli*. Figure 10

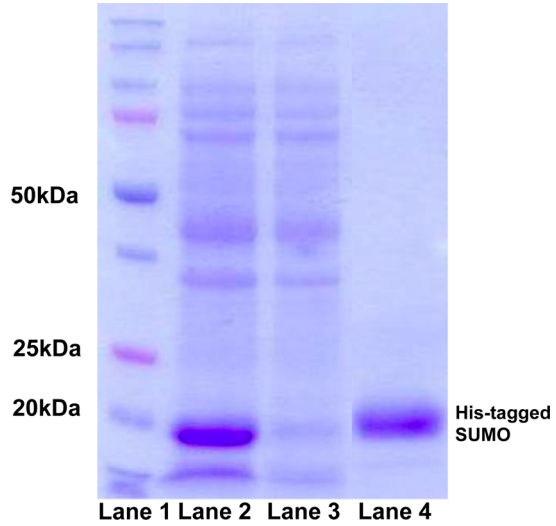

Figure 10. SDS-PAGE analysis of purification of overexpressed His-tagged SUMO protein from an *E. coli* lysate. Lane 1, molecular marker; Lane 2, cell lysate containing His-tagged SUMO protein; Lane 3, the cell lysate after passing through a (PAH/CMPEI)-Ni^{2+}-modified CM membrane; Lane 4, the eluate of the loaded membrane. Figure S9 (Supporting Information) shows the complete original gel.

shows the SDS-PAGE analysis of a cell extract that contained His-tagged SUMO (lane 2), the same cell extract after passing through a (PAH/CMPEI)-modified CM membrane (lane 3), and the eluate (lane 4) from the membrane loaded with the cell extract. Notably, the effluent of the loading solution contains minimal His-tagged SUMO protein, and the only detectable band from the eluate stems from the His-tagged SUMO protein. Thus, the membranes selectively capture His-tagged protein.

3.7. Metal-Ion Leaching. Low metal-ion leaching is sometimes important to avoid contaminating protein solutions. Thus, we examined leaching from several modified membranes and a common commercial Ni^{2+} column. Membranes modified with one and two bilayers of PAH/CMPEI-Ni^{2+} or PAH/PDCMAA-Ni^{2+} (deposited at pH 2 in 0.5 M NaCl) were washed with 5 mL each (160 bed volumes) of binding buffer 2, washing buffer 1, washing buffer 2, stripping buffer, and 2% HNO_3. (We summed the amounts of Ni^{2+} in the stripping buffer and HNO_3.) The GE Hitrap FF Ni column with a 1 mL bed volume was washed with 160 mL (160 bed volumes) each of binding buffer 2 and washing buffers 1 and 2. Subsequently, the remaining Ni^{2+} was eluted from the column with 15 mL of stripping buffer (elution was complete with EDTA, so 2% HNO_3 was not needed). All the solutions were analyzed by atomic absorption spectroscopy.

Table 1 shows the leaching from the GE Hitrap FF Ni column and different membranes as a percentage of the total Ni^{2+} binding. The (PAH/CMPEI)- and $(PAH/CMPEI)_2$-modified membranes show the least percentage leaching in the binding and washing buffers, and the percentage of leaching in the elution buffer is within a factor of ~2 for all systems, although the GE column shows the lowest leaching in that

DOI: 10.1021/am507607j
ACS Appl. Mater. Interfaces 2015, 7, 2575−2584

Table 1. Ni^{2+} Leaching from a GE Hitrap FF Ni Column and CM Nylon Membranes Modified with (PAH/PDCMAA), (PAH/PDCMAA)$_2$, (PAH/CMPEI), and (PAH/CMPEI)$_2$ Films[a]

	binding buffer 2	wash 1	wash 2	elution buffer	stripping buffer and 2% HNO_3
GE column (%)	30.7 ± 2.4	7.6 ± 0.8	7.5 ± 0.6	16.9 ± 1.1	37.2 ± 0.5
(PAH/PDCMAA) (%)	14.3 ± 4.0	6.5 ± 0.2	13.6 ± 0.1	14.8 ± 1.8	30.7 ± 2.2
(PAH/PDCMAA)$_2$ (%)	6.9 ± 0.9	4.4 ± 0.3	6.2 ± 0.1	31.0 ± 3.6	52.4 ± 4.7
(PAH/CMPEI) (%)	0.7 ± 1.3	2.0 ± 1.4	4.7 ± 1.5	34.7 ± 2.5	57.8 ± 4.0
(PAH/CMPEI)$_2$ (%)	0.7 ± 0.1	0.3 ± 0.6	1.7 ± 0.4	21.8 ± 3.4	75.4 ± 2.4

[a]The numbers represent the percentage of Ni^{2+} ion lost in each solution. All the substrates were treated with 160 bed volumes (each) of binding buffer 2, washing buffers 1 and 2, elution buffer, and stripping buffer. The experiment was repeated twice for all substrates, and uncertainties are differences between two trials.

buffer. The low leaching in the elution buffer for the GE column partly reflects the high leaching in the binding buffer. For all systems, the higher leaching in the elution buffer (0.5 M imidazole) than in the washing buffers stems from the formation of imidazole-Ni^{2+} complexes. Nevertheless, all the membrane substrates had less than 10 ppm of Ni^{2+} in the 5 mL of elution buffer except the membrane modified with (PAH/PDCMAA)$_2$, which had 12.9 ± 1.1 ppm of Ni^{2+}. (Note the values in Table 1 are percentages of the total Ni^{2+} loaded and not concentrations.) The Ni^{2+} binding capacity of the GE Hitrap FF Ni column is 1.6 ± 0.2 mg/mL, and Figure 6 shows that the Ni^{2+} binding capacities for all the membranes are higher than that for the Ni column. (For example, the Ni^{2+} binding capacity of the (PAH/CMPEI)-modified membrane is 2.7 mg/mL.) Overall, the metal leaching from all the substrates is similar, which is not surprising given that they likely have related ligands.

3.8. Film Stability and Reusability. Adsorption of (PAH/CMPEI)-Ni^{2+} films may prove sufficiently simple and inexpensive to provide disposable, functional membranes. However, membrane reuse is always desirable, and the high swelling of PAH/CMPEI films (as much as 680%, see section 3.2) in buffer may lead to partial polyelectrolyte desorption. We evaluated the stability of CMPEI-containing films both on wafers and in membranes. For (PAH/CMPEI)$_2$ films on Au-coated Si wafers (deposited on a MPA monolayer at pH 2 in 0.5 M NaCl), immersion for 20 h in binding buffer 2 (pH 7.4) led to only a 10% decrease in thickness, most of which occurred in the first 4 h (see Figure S10, Supporting Information). Absorbances in reflectance IR spectroscopy also decreased about 10%, suggesting that the change in thickness results from a small loss of film and not simply deswelling or a change in conformation.

Using TOC analysis, we determined the amount of the polyelectrolyte film lost during passage of binding buffer 2 (pH 7.4) through a membrane. After forming a (PAH/CMPEI) film and rinsing with only water, the first 20 mL of washing buffer passed through the membrane contained around 4 ppm of polymer (we assumed that the leaching was only due to CMPEI and used 1−10 ppm of CMPEI solutions as standards). This corresponds to <20% of the total polymer based on our estimate of 14 mg of CMPEI/mL of membrane (the membrane volume in these leaching studies was 0.035 cm^3, diameter 2 cm). Subsequent buffer washes contained <0.005 ppm (TOC detection limit) of polymer. Additionally, we added wash solutions to the Bradford dye and tested the absorbance at 595 nm (Figure S11, Supporting Information) as in a typical Bradford assay. The first milliliter of washing solution gave an absorbance of 0.02, which is equivalent to the absorbance given by 0.03 mg/mL of Con A. This absorbance rapidly declines and was only 0.002 after passing 20 mL of washing buffer through the membrane. In a typical protein-binding test, we wash the membranes with 40 mL of binding buffer prior to loading protein. However, some breakthrough curves such as that for (PAH/CMPEI)$_2$-Cu^{2+} (Figure S8, Suppporting Information) show a small and decreasing Bradford assay signal over the first 1−2 mL of protein loading. This may indicate that protein replaces a small amount of polyelectrolyte, i.e., the initial loading solution might contain 5 ppm of polyelectrolyte after passing through the membrane. We did not see this issue in binding of His U. As a further test of membrane stability, we performed four cycles of loading and elution of Con A in (PAH/CMPEI)-Cu^{2+}-modified CM membranes. The Con A binding decreased by 40% (from 58 to 35 mg/mL) over four cycles of loading, recharging with Cu^{2+}, and elution (Figure S12, Supporting Information). Thus, reuse is possible, but performance declines with use.

4. CONCLUSION

This study presents a facile method, LbL adsorption of functional polyelectrolytes, to modify membranes with metal-ion complexes that selectively capture His-tagged proteins. PAH/CMPEI adsorption yields a membrane with a His-tagged ubiquitin binding capacity of ∼60 mg/mL, which is equal to the capacity of high-binding commercial beads. Moreover, these (PAH/CMPEI)-modified membranes show less than 10 ppm of Ni^{2+} in the elution buffer (0.5 M imidazole). Membranes modified with PAH/CMPEI show about 2 times the protein binding of corresponding membranes modified with PAH/PDCMAA, presumably because of more swelling with PAH/CMPEI. The His-tagged protein-binding capacity of the (PAH/PEI)-Ni^{2+}-modified membranes is 2/3 of that for membranes modified through growth of polymer brushes or LbL adsorption of PAA/PEI/PAA followed by derivatization. However, direct adsorption of PAH and CMPEI in membranes is much simpler and less expensive than previous membrane modification methods and may lead to inexpensive, disposable membranes for rapid purification of His-tagged protein.

■ ASSOCIATED CONTENT

Supporting Information

CMPEI synthesis and characterization, protein breakthrough curves, XPS data, reflectance FTIR spectra, original gel electrophoresis, additional data on film stability and swelling, experimental details for atomic absorption spectroscopy, and TOC analysis. This material is available free of charge via the Internet at http://pubs.acs.org.

DOI: 10.1021/am507607j
ACS Appl. Mater. Interfaces 2015, 7, 2575−2584

AUTHOR INFORMATION

Corresponding Author

*M. L. Bruening. E-mail: bruening@chemistry.msu.edu.

Notes

The authors declare no competing financial interest.

ACKNOWLEDGMENTS

We are grateful to the U.S. National Science Foundation (CHE-1152762) for funding this work. We thank Yanlyang Pan for helping with TOC analysis, Stacy Hovde for providing cell lysates with His-SUMO protein, and Per Askeland for XPS analysis.

REFERENCES

(1) Lichty, J. J.; Malecki, J. L.; Agnew, H. D.; Michelson-Horowitz, D. J.; Tan, S. Comparison of Affinity Tags for Protein Purification. *Protein Express. Purif.* **2005**, *41*, 98−105.

(2) Porath, J. Immobilized Metal-Ion Affinity-Chromatography. *Protein Express. Purif.* **1992**, *3*, 263−281.

(3) Arnau, J.; Lauritzen, C.; Petersen, G. E.; Pedersen, J. Current Strategies for the Use of Affinity Tags and Tag Removal for the Purification of Recombinant Proteins. *Protein Express. Purif.* **2006**, *48*, 1−13.

(4) Kawai, T.; Saito, K.; Lee, W. Protein Binding to Polymer Brush, Based on Ion-Exchange, Hydrophobic, and Affinity Interactions. *J. Chromatogr. B: Anal. Technol. Biomed. Life Sci.* **2003**, *790*, 131−142.

(5) Bhut, B. V.; Husson, S. M. Dramatic Performance Improvement of Weak Anion-Exchange Membranes for Chromatographic Bioseparations. *J. Membr. Sci.* **2009**, *337*, 215−223.

(6) Ghosh, R. Protein Separation Using Membrane Chromatography: Opportunities and Challenges. *J. Chromatogr. A* **2002**, *952*, 13−27.

(7) Datta, S.; Bhattacharyya, D.; Ray, P. D.; Nath, A.; Toborek, M. Effect of Pre-Filtration on Selective Isolation of Tat Protein by Affinity Membrane Separation: Analysis of Flux, Separation Efficiency, and Processing Time. *Sep. Sci. Technol.* **2007**, *42*, 2451−2471.

(8) Wang, J.; Sproul, R. T.; Anderson, L. S.; Husson, S. M. Development of Multimodal Membrane Adsorbers for Antibody Purification Using Atom Transfer Radical Polymerization. *Polymer* **2014**, *55*, 1404−1411.

(9) Yin, D. X.; Ulbricht, M. Antibody-Imprinted Membrane Adsorber Via Two-Step Surface Grafting. *Biomacromolecules* **2013**, *14*, 4489−4496.

(10) Thommes, J.; Etzel, M. Alternatives to Chromatographic Separations. *Biotechnol. Prog.* **2007**, *23*, 42−45.

(11) Roper, D. K.; Lightfoot, E. N. Separation of Biomolecules Using Adsorptive Membranes. *J. Chromatogr. A* **1995**, *702*, 3−26.

(12) Thommes, J.; Kula, M. R. Membrane Chromatography - An Integrative Concept in the Downstream Processing of Proteins. *Biotechnol. Prog.* **1995**, *11*, 357−367.

(13) Saxena, A.; Tripathi, B. P.; Kumar, M.; Shahi, V. K. Membrane-based Techniques for the Separation and Purification of Proteins: An Overview. *Adv. Colloid Interface Sci.* **2009**, *145*, 1−22.

(14) Zeng, X. F.; Ruckenstein, E. Membrane Chromatography: Preparation and Applications to Protein Separation. *Biotechnol. Prog.* **1999**, *15*, 1003−1019.

(15) Sun, L.; Dai, J. H.; Baker, G. L.; Bruening, M. L. High-Capacity, Protein-Binding Membranes Based on Polymer Brushes Grown in Porous Substrates. *Chem. Mater.* **2006**, *18*, 4033−4039.

(16) Bhut, B. V.; Conrad, K. A.; Husson, S. M. Preparation of High-Performance Membrane Adsorbers by Surface-Initiated AGET ATRP in the Presence of Dissolved Oxygen and Low Catalyst Concentration. *J. Membr. Sci.* **2012**, *390*, 43−47.

(17) Yang, Q.; Ulbricht, M. Cylindrical Membrane Pores with Well-Defined Grafted Linear and Comblike Glycopolymer Layers for Lectin Binding. *Macromolecules* **2011**, *44*, 1303−1310.

(18) Kawakita, H.; Masunaga, H.; Nomura, K.; Uezu, K.; Akiba, I.; Tsuneda, S. Adsorption of Bovine Serum Albumin to a Polymer Brush Prepared by Atom-Transfer Radical Polymerization in a Porous Inorganic Membrane. *J. Porous Mater.* **2007**, *14*, 387−391.

(19) Honjo, T.; Hoe, K.; Tabayashi, S.; Tanaka, T.; Shimada, J.; Goto, M.; Matsuyama, H.; Maruyama, T. Preparation of Affinity Membranes Using Thermally Induced Phase Separation for One-Step Purification of Recombinant Proteins. *Anal. Biochem.* **2013**, *434*, 269−274.

(20) Bhut, B. V.; Wickramasinghe, S. R.; Husson, S. M. Preparation of High-Capacity, Weak Anion-Exchange Membranes for Protein Separations Using Surface-Initiated Atom Transfer Radical Polymerization. *J. Membr. Sci.* **2008**, *325*, 176−183.

(21) Ulbricht, M.; Yang, H. Porous Polypropylene Membranes with Different Carboxyl Polymer Brush Layers for Reversible Protein Binding Via Surface-Initiated Graft Copolymerization. *Chem. Mater.* **2005**, *17*, 2622−2631.

(22) Bhattacharjee, S.; Dong, J. L.; Ma, Y. D.; Hovde, S.; Geiger, J. H.; Baker, G. L.; Bruening, M. L. Formation of High-Capacity Protein-Adsorbing Membranes through Simple Adsorption of Poly(acrylic acid)-Containing Films at Low pH. *Langmuir* **2012**, *28*, 6885−6892.

(23) Naka, K.; Tachiyama, Y.; Hagihara, K.; Tanaka, Y.; Yoshimoto, M.; Ohki, A.; Maeda, S. Synthesis and Chelating Properties of Poly(*N*,*N*-dicarboxymethyl)allylamine Derived from Poly(allylamine). *Polym. Bull.* **1995**, *35*, 659−663.

(24) Sheng, C. J.; Wijeratne, S.; Cheng, C.; Baker, G. L.; Bruening, M. L. Facilitated Ion Transport through Polyelectrolyte Multilayer Films Containing Metal-Binding Ligands. *J. Membr. Sci.* **2014**, *459*, 169−176.

(25) Wijeratne, S.; Bruening, M. L.; Baker, G. L. Layer-by-Layer Assembly of Thick, Cu^{2+}-Chelating Films. *Langmuir* **2013**, *29*, 12720−12729.

(26) Anzai, J.; Kobayashi, Y.; Nakamura, N.; Nishimura, M.; Hoshi, T. Layer-by-Layer Construction of Multilayer Thin Films Composed of Avidin and Biotin-Labeled Poly(amine)s. *Langmuir* **1999**, *15*, 221−226.

(27) Ni-NTA Agarose Specifications. http://www.qiagen.com/us/products/catalog/sample-technologies/protein-sample-technologies/purification-kits-and-resins/ni-nta-agarose/#technicalspecification (accessed December 29, 2014).

(28) His60 Nickel Resin Beats Ni-NTA Resin for His-Tag Purification. http://www.clontech.com/US/Support/Applications/Tagged_Protein_Purification/Ni-NTA_Resin_vs_His60 (accessed December 29, 2014).

(29) Bucur, C. B.; Sui, Z.; Schlenoff, J. B. Ideal Mixing in Polyelectrolyte Complexes and Multilayers: Entropy Driven Assembly. *J. Am. Chem. Soc.* **2006**, *128*, 13690−13691.

(30) Vig, J. R. UV Ozone Cleaning of Surfaces. *J. Vac. Sci. Technol., A* **1985**, *3*, 1027−1034.

(31) Miller, M. D.; Bruening, M. L. Correlation of the Swelling and Permeability of Polyelectrolyte Multilayer Films. *Chem. Mater.* **2005**, *17*, 5375−5381.

(32) Dai, J. H.; Bao, Z. Y.; Sun, L.; Hong, S. U.; Baker, G. L.; Bruening, M. L. High-Capacity Binding of Proteins by Poly(acrylic acid) Brushes and Their Derivatives. *Langmuir* **2006**, *22*, 4274−4281.

(33) Nakamoto, K.; Morimoto, Y.; Martell, A. E. Infrared Spectra of Aqueous Solutions. 2. Iminodiacetic Acid, *N*-Hydroxyethyliminodiacetic Acid and Nitrilotriacetic Acid. *J. Am. Chem. Soc.* **1962**, *84*, 2081−2084.

(34) Pack, D. W.; Arnold, F. H. Langmuir Monolayer Characterization of Metal Chelating Lipids for Protein Targeting to Membranes. *Chem. Phys. Lipids* **1997**, *86*, 135−152.

(35) Hoffmann, K.; Tieke, B. Layer-by-Layer Assembled Membranes Containing Hexacyclen-Hexaacetic Acid and Polyethyleneimine *N*-Acetic Acid and Their Ion Selective Permeation Behaviour. *J. Membr. Sci.* **2009**, *341*, 261−267.

(36) McAloney, R. A.; Sinyor, M.; Dudnik, V.; Goh, M. C. Atomic Force Microscopy Studies of Salt Effects on Polyelectrolyte Multilayer Film Morphology. *Langmuir* **2001**, *17*, 6655−6663.

DOI: 10.1021/am507607j
ACS Appl. Mater. Interfaces 2015, 7, 2575−2584

(37) Schlenoff, J. B.; Dubas, S. T. Mechanism of Polyelectrolyte Multilayer Growth: Charge Overcompensation and Distribution. *Macromolecules* **2001**, *34*, 592−598.
(38) Dobrynin, A. V.; Rubinstein, M.; Joanny, J. F. Adsorption of a Polyampholyte Chain on a Charged Surface. *Macromolecules* **1997**, *30*, 4332−4341.
(39) Jeon, J.; Dobrynin, A. V. Monte Carlo Simulations of Polyampholyte-Polyelectrolyte Complexes: Effect of Charge Sequence and Strength of Electrostatic Interactions. *Phys. Rev. E* **2003**, *67*.
(40) Bowman, W. A.; Rubinstein, M.; Tan, J. S. Polyelectrolyte-Gelatin Complexation: Light-Scattering Study. *Macromolecules* **1997**, *30*, 3262−3270.
(41) Fu, J. H.; Ji, J.; Shen, L. Y.; Kueller, A.; Rosenhahn, A.; Shen, J. C.; Grunze, M. pH-Amplified Exponential Growth Multilayers: A Facile Method to Develop Hierarchical Micro- and Nanostructured Surfaces. *Langmuir* **2009**, *25*, 672−675.
(42) Bieker, P.; Schönhoff, M. Linear and Exponential Growth Regimes of Multi Layers of Weak Polyelectrolytes in Dependence on pH. *Macromolecules* **2010**, *43*, 5052−5059.
(43) Becker, J. W.; Reeke, G. N.; Wang, J. L.; Cunningham, B. A.; Edelman, G. M. Covalent and 3-Dimensional Structure of Concanavalin-A. 3. Structure of Monomer and Its Interactions with Metals and Saccharides. *J. Biol. Chem.* **1975**, *250*, 1513−1524.
(44) Anuraj, N.; Bhattacharjee, S.; Geiger, J. H.; Baker, G. L.; Bruening, M. L. An All-Aqueous Route to Polymer Brush-Modified Membranes with Remarkable Permeabilites and Protein Capture Rates. *J. Membr. Sci.* **2012**, *389*, 117−125.

DOI: 10.1021/am507607j
ACS Appl. Mater. Interfaces 2015, 7, 2575−2584